Cationic Doping Engineering of ZnV_2O_4 Cathode toward Fast Zn^{2+} Storage

Xiaoqing Liu [a, b, *], Mengmeng Bai [a], Ruimiao Si [a], Shun Zhou [a], Chuang Yu [c], Jinjiang Wu [a, *], Longlong Dong [d], Youzhi Liu [a, b, *]

[a] School of Chemistry and Chemical Engineering, North University of China; Taiyuan 030051, China, E-mail: sa175010@mail.ustc.edu.cn

[b] Shanxi Province Key Laboratory of Chemical Process Intensification, North University of China, Taiyuan 030051, China, E-mail: 20220194@nuc.edu.cn, liuyz@nuc.edu.cn

[c] School of Information Mechanics and Sensing Engineering, Xidian University, Xi' an, Shaanxi 710126, China

[d] Inner Mongolia Research Institute of Synthetic Chemical Industry, Hohhot, 010010, China

Experimental Section

Chemical

Vanadium oxide (V_2O_5, 99.5%) was acquired from 3A, zinc acetate ($Zn(CH_3COO)_2 \cdot 2H_2O$, 99%), hydrazine hydrate (N_2H_4, 99%), and aluminium acetate ($Al(CH_3COO)_3 \cdot 9H_2O$, AR) were bought from Sinopharm Chemical Reagent Corp.

Synthesis of Al doped ZnV_2O_4 sample

1 mmol $Zn(CH_3COO)_2 \cdot 2H_2O$ and 1 mmol V_2O_5 were dispersed into 30 mL deionized water. Next, 1 mL N_2H_4 was added and stirred for 1 h. Subsequently, 0.04 mmol $Al(CH_3COO)_3 \cdot 9H_2O$ was introduced, followed by stirring for 30 min. The mixture was sealed in a 50 mL autoclave, heated to 180 °C and maintained for 15 h. The resulting products were then thoroughly washed with deionized water and ethanol (three times each), followed by drying at 60 °C overnight. The resulting material was designated as Al-ZVO.

Synthesis of ZnV_2O_4 sample

ZnV_2O_4 was synthesized similarly to Al-ZVO, but without the addition of $Al(CH_3COO)_3 \cdot 9H_2O$. The resulting sample was designated as ZVO.

Characterization

Sample morphology was observed by scanning electron microscopy (SEM, TESCAN MIRA LMS, Czech Republic). The microstructure of Al-ZVO was examined using transmission electron microscopy (TEM, JEOL JEM-F200). The structure was analyzed by powder X-ray diffraction (XRD, Dandong Haoyuan-DX-2700BH). Surface chemical valence was determined by X-ray photoelectron spectroscopy (XPS, Thermo Scientific ESCALAB 250Xi).

Electrochemical measurements

An electrode slurry comprising Al-ZVO, super P, and polyvinylidene fluoride (PVDF) in a weight ratio of 7:2:1. The slurry was coated onto 14 mm diameter stainless steel substrates. CR2025 coin cells were assembled using the coated electrodes as the cathode, zinc foil (thickness of 0.07 mm) and Whatman GF/D was used as counter electrode and separator, respectively. The 3M $Zn(CF_3SO_3)_2$ aqueous solution is used as electrolyte with a volume of 50 μL for battery assembly. The loading of test electrodes is 1.4 ~ 2.5 mg cm^{-2}. The average thickness of the electrode is 20 μm. Electrochemical performance was evaluated using a Neware Battery Test System.

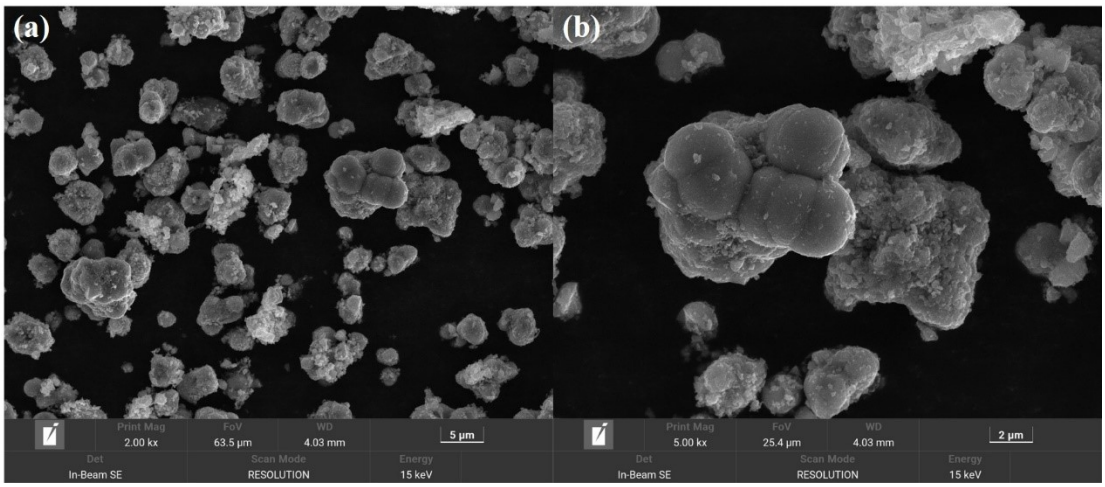

Figure S1. (a-b) SEM images for ZnV_2O_4 sample.

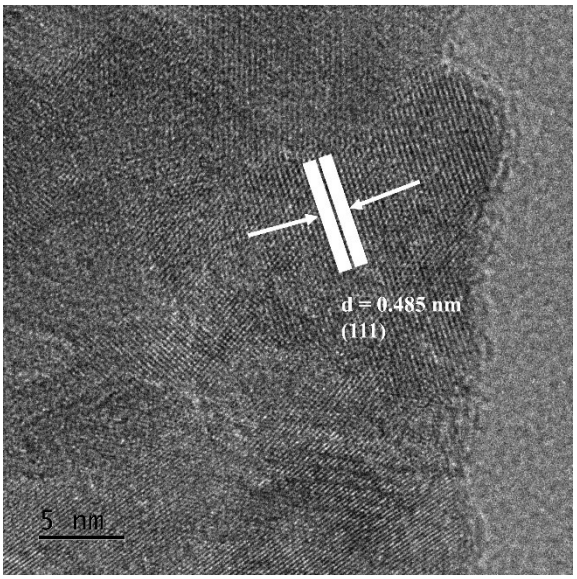

Figure S2. TEM images of ZVO sample.

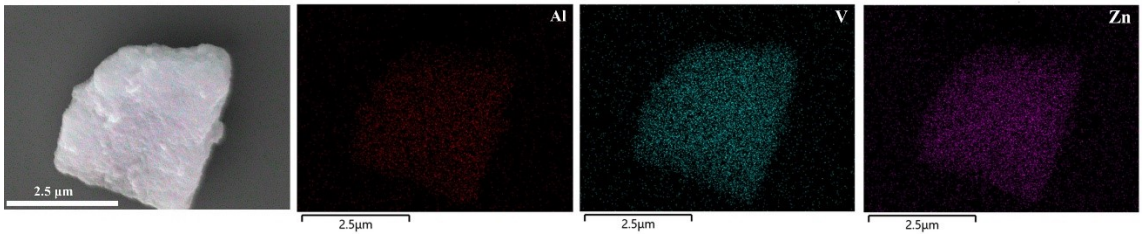

Figure S3. SEM Mapping of Al-ZVO sample.

Table S1. Charge transfer resistance for Al-ZVO and ZVO samples.

Sample	Al-ZVO	ZVO	Error (%)
R_s (Ω)	0.76	1.9	0.9
R_{ct} (Ω)	85	110	1.5

The equivalent circuit model shown in Figure 3f was selected to physically represent the electrochemical interfaces and processes in our system. It comprises R_s to describe ohmic resistance originated from contact resistance of components in the high frequency range, and R_{ct} to model the charge transfer resistance in the mid-frequency range as well as W_1 related to the Zn^{2+} diffusion in the electrode within low-frequency range. This model is well-established for intercalation-type cathode materials systems and provided an excellent fit to the experimental data across the entire frequency range.

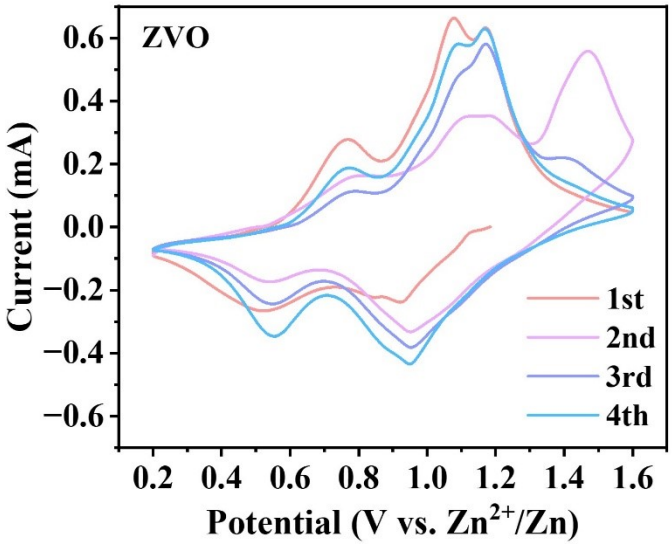

Figure S4. CV curves of ZVO cathode.

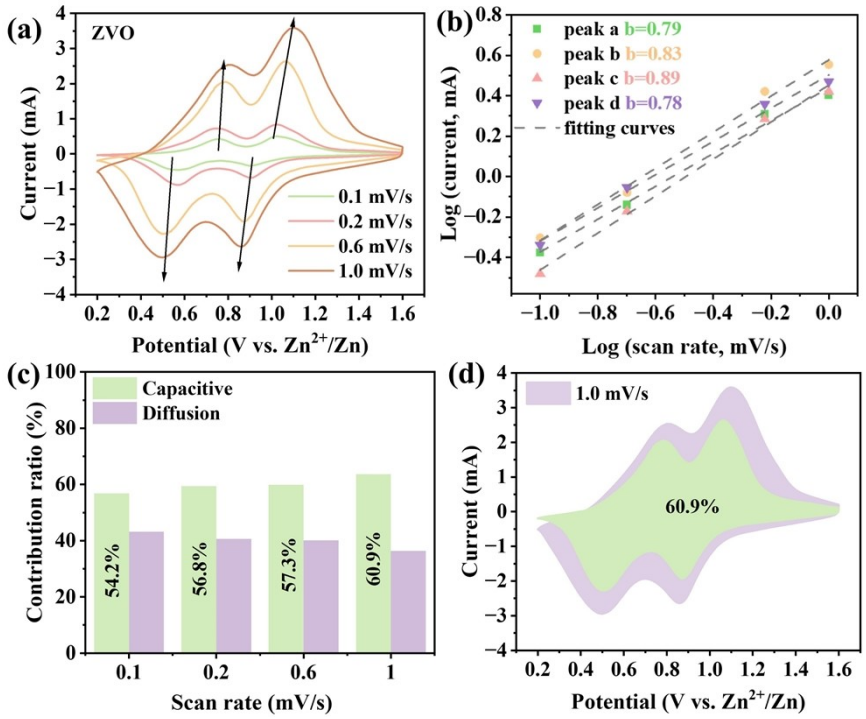

Figure S5. The electrochemical kinetics of ZVO cathode: (a) CV curves at 0.1, 0.2, 0.6 and 1.0 mV s^{-1}, (b) log (scan rate) ~ log (*i*), (c) bar chart of capacitive and diffusion contributions, (d) capacitive (green) and diffusion (purple) contributions at 1.0 mV/s.

Table S2. Comparison of electrochemical performance of Al-ZnV_2O_4 cathode with other spinel oxides.

Sample	Cycling performance	Rate capability	References
ZMn_2O_4/C	80 mA h g^{-1} after 500 cycles at 0.5 A g^{-1}	-	[1]
MgV_2O_4	128.9 mA h g^{-1} after 500 cycles at 4.0 A g^{-1}	176 mA h g^{-1} at 5 A g^{-1}	[2]
ZnV_2O_4	206 mAh g^{-1} over 1000 cycles at a 10 C	174 mA h g^{-1} at 20 C	[3]
Ni-$ZnMn_2O_4$	181 mA h g^{-1} after 100 cycles at 0.2 A g^{-1}	84 mA h g^{-1} at 2 A g^{-1}	[4]
MXene/$ZnMn_2O_4$	58 mA h g^{-1} after 2000 cycles at 1 A g^{-1}	84 mA h g^{-1} at 4 A g^{-1}	[5]
Ni/Co-$ZnMn_2O_4$@N-rGO	95.4 mA h g^{-1} after 900 cycles at 1 A g^{-1}	94 mA h g^{-1} at 1.5 A g^{-1}	[6]
Mg_2VO_4	74 mA h g^{-1} after 1000 cycles at 1 A g^{-1}	125 mA h g^{-1} at 2 A g^{-1}	[7]
$ZnMn_2O_4 \cdot 0.94H_2O$	77 mA h g^{-1} after 2000 cycles at 4 A g^{-1}	28 mA h g^{-1} at 8 A g^{-1}	[8]
$MnCo_2O_4$	81 mA h g^{-1} after 250 cycles at 0.2 A g^{-1}	175 mA h g^{-1} at 1 A g^{-1}	[9]
Mn_3O_4	245 mA h g^{-1} after 500 cycles at 0.5 A g^{-1}	126 mA h g^{-1} at 1.5 A g^{-1}	[10]
Al-ZnV_2O_4	147 mA h g^{-1} after 940 cycles at 5 A g^{-1}	91 mA h g^{-1} at 20 A g^{-1}	**This work**

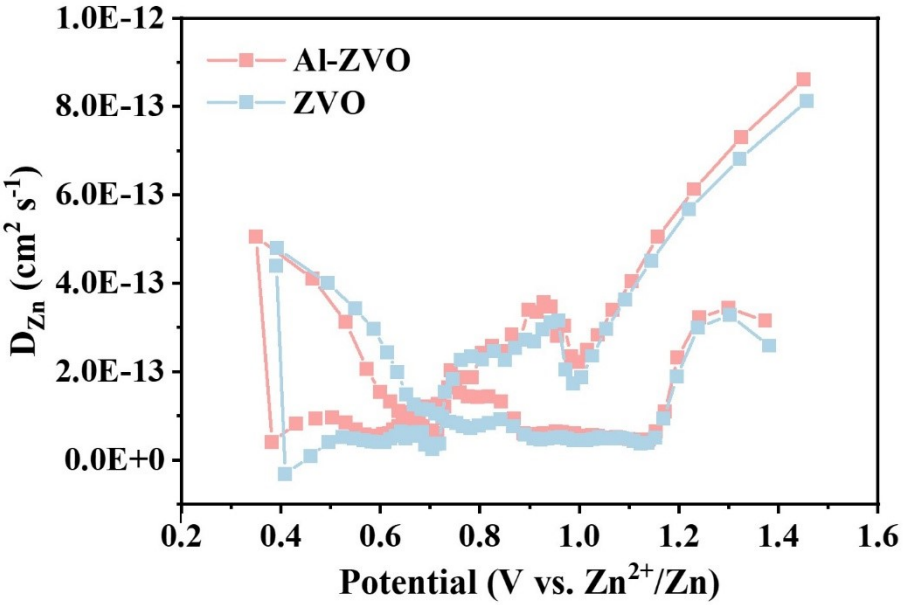

Figure S6. D_{Zn} for ZVO and Al-ZVO samples.

References:

[1] Ning Zhang, Fangyi Cheng, Yongchang Liu, et al., Cation-deficient spinel $ZnMn_2O_4$ cathode in $Zn(CF_3SO_3)_2$ electrolyte for rechargeable aqueous Zn-ion battery, J. Am. Chem. Soc., 2016, 138, 12894−12901.

[2] Wen Tang, Binxu Lan, Chen Tang, et al., Urchin-like spinel MgV_2O_4 as a cathode material for aqueous zinc ion batteries, ACS Sustainable Chem. Eng., 2020, 8, 3681−3688.

[3] Yi Liu, Chang Li, Jia Xu, et al., Electro activation-induced spinel ZnV_2O_4 as a high-performance cathode material for aqueous zinc-ion battery, Nano Energy 2020, 67, 104211.

[4] Chuan Wang, Bo-Hao Xiao, Jiale Huang, et al., Microstructure strain of $ZnMn_2O_4$ spinel by regulation of tetrahedral sites for high-performance aqueous zinc-ion battery, Adv. Funct. Mater., 2024, 34, 2405680.

[5] Minjie Shi, Bei Wang, Yi Shen, 3D assembly of MXene-stabilized spinel $ZnMn_2O_4$ for highly durable aqueous zinc-ion batteries, Chemical. Eng. Journal, 2020, 399, 125627.

[6] Yayuan Tao, Zhi Li, Linbin Tang, Nickel and cobalt Co-substituted spinel $ZnMn_2O_4$@N-rGO for increased capacity and stability as a cathode material for rechargeable aqueous zinc-ion battery, Electrochim. Acta, 2020, 331, 135296.

[7] Yu Zhang, Jing Xu, Chenfan Liu, et al., Ion-exchange-induced high-performance of inverse spinel Mg_2VO_4 for aqueous zinc-ion batteries, 2022, 549, 232075.

[8] Tzu-Ho Wu and Wei-Yuan Liang, Reduced intercalation energy barrier by rich structural water in spinel $ZnMn_2O_4$ for high-rate zinc-ion batteries, ACS Appl. Mater. Interfaces, 2021, 13, 20, 23822–23832.

[9] Nishant Yadav, Sonti Khamsanga, Soorathep Kheawhom, $MnCo_2O_4$ spinel microsphere assembled with flake structure as a cathode for high-performance zinc ion battery, Journal of Energy Storage, 2023, 64, 107148.

[10] Le Jiang, Zeyi Wu, Yanan Wang, et al., Ultrafast zinc-ion diffusion ability observed in 6.0-nanometer spinel nanodots, ACS Nano, 2019, 13, 9, 10376–10385.